Paper AAS 05-257

Drag Coefficient Variability at 175-500 km from the Orbit Decay Analyses of Spheres

Bruce R. Bowman
Air Force Space Command
Space Analysis Division

Kenneth Moe
Science and Technology Corp.

AAS/AIAA Astrodynamics Specialists Conference

Lake Tahoe, CA, August 7-11, 2005

AAS Publications Office, P.O. Box 28130, San Diego, CA 92198

AAS 05-257

Drag Coefficient Variability at 175-500 km from the Orbit Decay Analyses of Spheres

Bruce R. Bowman*
Air Force Space Command
Space Analysis Division/XPY
bruce.bowman@peterson.af.mil
719-556-3710

Kenneth Moe
Science and Technology Corp.
kmmoe@att.net
(949) 509-1955

In the past it has been customary to use the drag coefficient 2.2 for satellites of compact shapes when calculating absolute atmospheric densities. This assumption has introduced a bias into thermospheric density models. In this paper we evaluate that bias observed in the Jacchia 70 model. Newly developed methods have made possible precise analyses of the orbital behavior of satellites, with the ability to determine improved fitted drag coefficients and their variability. A new density determination method was used to compute drag coefficients from the decay of the ODERACS spheres, the Starshine spheres, several radar calibration Calspheres, GFZ-1, and numerous Russian Taifun radar calibration spheres. Atmospheric temperature and density corrections were first determined on a daily basis using up to 79 calibration satellites in the height range of 150-500 km. These corrections were then applied to special perturbation differential orbit corrections for all the decayed spheres. The resulting ballistic coefficient (B) values were then used to deduce the variation of the fitted drag coefficient values during the last few hundred days of decay. Previous analyses from a few specialized satellites have in the past yielded some information on energy accommodation and angular distributions of molecules reemitted from satellite surfaces. Such information has made possible the calculation of physical drag coefficients from the momentum transferred to the satellite. In the present paper we compare the two types of drag coefficient, the observed and computed physical coefficients. This comparison enables us to calculate the dependence of drag coefficients on satellite altitude. It is also determined that the Jacchia 70 density model, on average, is too high by 8% at 200 km, increasing to 13 % at 500 km.

Introduction

The US Air Force has long supported efforts to improve satellite orbital predictions, in cooperation with the US Navy, NASA, the Harvard-Smithsonian Center for Astrophysics, and many universities and Air Force contractors. Over the years, the Air Force prediction efforts have evolved along two lines: (1) In the High Accuracy Satellite Drag Model (HASDM)[1] program many orbiting satellites are used to monitor the atmosphere and update an atmospheric model in real time; (2) In the DMSP Program, the spectroscopic sensors SSUSI and SSULI will monitor the atmosphere and update it. A

major objective of both these programs is to measure and predict absolute atmospheric densities. Improvement in the knowledge of drag coefficients contributes directly to that goal.

Better drag coefficients will also contribute to the improvement of thermospheric density models. A landmark in the effort to improve models was achieved by Marcos[2] in 1985 when he compared and evaluated 14 models against accelerometer measurements from seven satellites. A decade later, Chao et al.[3] used orbital data from the ODERACS I and ODERACS II families of spheres to measure the biases in the Jacchia 71 and the MSIS 90 density models near sunspot minimum. They accomplished this by comparing the fitted drag coefficient, $C_{D,}$ with the physical drag coefficient, $C_{DP,}$ calculated from the actual momentum transfer to the satellite. More recently, Owens[4] has revised and improved the Jacchia models to create the NASA Marshall Engineering Thermospheric Model –Version 2.0 (MET-V 2.0 Model). This model has been subjected to an extensive statistical evaluation by Wise et al[5].

Further recent progress[6] in the analysis of orbital data has refined the semiannual variation and other parameters of the Jacchia 70 thermospheric density model[7]. This new development has presented an opportunity to use the improved Jacchia model with data from spherical satellites to refine our knowledge of drag coefficients and improve the absolute densities in the model.

Analysis Method for Fitted Drag Coefficients

The method developed to determine accurate C_D values is to obtain accurate ballistic coefficient (B) values from special perturbation orbit fits using a corrected atmospheric model. In standard orbit fits the B values, equal to the drag coefficient times the area to mass ratio (C_DA/M), also contain unmodeled density variations from orbit fit aliasing, as well as contain other variations due to frontal area changes plus C_D changes. However, if a corrected atmospheric model can be used then this removes the aliasing of the unmodeled density variations into the B variations. The corrected model is based on calibrating the atmosphere on a daily basis from analysis of daily temperature and density corrections on many satellites over the time period of interest. Once the atmospheric model has been corrected (on a daily basis) the model is then used to obtain accurate B values. The resulting B variations can then be attributed solely to C_D variations for spherical satellites which have no frontal area problems.

Atmospheric Model Corrections

Daily temperature corrections to the HASDM modified Jacchia 1970 atmospheric model have been obtained on 79 calibration satellites for the period 1994 through 2003, and 35 calibration satellites for the solar maximum period 1989 through 1990. All the "calibration" satellites are moderate to high eccentricity, with perigee heights ranging from 150 to 500 km. Figure 1 shows the satellites grouped by perigee height and inclination for the 1994-2003 period.

Height Km:	150 200	200 250	250 300	300 400	400 500	**Total**
Inclination						
20-30	1	3	4	6	3	17
30-40	23	3	2	1	1	30
40-50	6		1			7
50-60		1				1
60-70					1	1
70-80			1	2		3
80-100			2	12	6	20
Total	30	7	10	21	11	**79**

Figure 1. Calibration satellite orbits as a function of height and inclination bands.

The daily correction values were obtained using a special energy dissipation rate (EDR) method[8], where radar and optical observations are fit with special orbit perturbations. It has been shown that using this method results in daily average density values (representing drag at perigee) accurate to 2-4% during solar maximum conditions. The first step was to correct the local solar time and latitude equations in the atmospheric model. This was accomplished by least squares fitting all the daily values over the 1994 through 2003 period, obtaining corrections as a function of local solar time and latitude for different heights and solar EUV activity. The next step was to use all the calibration satellites daily temperature corrections, and on a daily basis, least squares fit the values to form a daily global temperature correction field as a function of height.

The daily temperature correction equations obtained above were then used in the modified Jacchia 1970 atmospheric model to compute density values at every integration step during the orbit fits. To validate the temperature corrections orbit fits were obtained on 7 different validation orbits from 1994 through 2003. The validation orbits were chosen to have moderate to high eccentricity in order that the perigee heights would remain almost constant during the entire 10-year evaluation period. B values were obtained from the daily orbit fits, first without the temperature corrections, and then with the temperature corrections. Standard deviation (STD) values were then obtained on the B values with and without the corrections. If the temperature corrections are perfect then the B variations should be very small after applying the corrections. Table 1 lists the validation satellites with the STD results. The STD values show a very significant reduction. Note that the STD on the B values for the non-corrected data corresponds mainly to unmodeled density variations, which increase as the height increases. This has been observed repeatedly from previous HASDM analyses. Finally, the significant reduction in B STD values demonstrates the validity of the computed daily temperature corrections.

Satellite	Name	Inc	Per. Ht	Apg. Ht	94-97 B STD	98-02 B STD		94-97 B STD	98-02 B STD
		(deg)	(km)	(km)	% (No dTc)	% (No dTc)		% (dTc used)	% (dTc used)
26692	PAM-D R/B	38.7	175	5300	-----	8.3		-----	4.7
06073	Spheriod	52.1	210	5000	10.1	8.1		5.4	3.9
22875	Taifun Sphere	83.0	300	1550	11.8	11.0		5.9	4.5
12138	Taifun Sphere	83.0	390	1725	15.0	16.1		8.0	4.8
14483	Taifun Sphere	82.9	390	1630	14.3	15.9		7.0	4.8
00060	Explorer 8	49.9	400	1150	14.2	15.2		6.7	4.2
00022	Explorer 7	50.3	525	825	14.0	21.6		9.1	5.5
				Ave:	**13.2 %**	**13.7 %**		**7.0 %**	**4.6 %**

Table 1. Validation satellites with standard deviations (STD) of B with and without daily temperature field corrections dTc. Periods of solar minimum (94-97) and solar maximum (98-02) are listed separately.

Determination of Physical Drag Coefficients

The mathematical models of physical drag coefficient C_{DP} that will be used in this paper were developed by Sentman[9,10] and Schamberg[11,12] at the beginning of the space age. Sentman's model was soon tested when the Air Force flew long cylindrical satellites, beginning in 1960. Although much of the early work was classified, the large drag coefficients calculated in Sentman's 1961 papers were confirmed by the data and analyses eventually published by Bruce[13] and by DeVries et al.[14]. In 1975, Imbro et al.[15] demonstrated the utility of Schamberg's model for investigating the effect of the angular distribution of reemitted molecules on the drag coefficient. In 1996 it was shown how the two models could be used together to calculate the effect of a completely diffuse distribution plus a quasi-specular fraction on the physical drag coefficients of a sphere and a cylinder[16]. These two models will be used in the present paper to calculate physical drag coefficients to compare with the fitted drag coefficients of spheres.

Marcos' 1985 survey[2] compared densities calculated from 14 thermospheric models with measurements by accelerometers aboard three long cylindrical satellites and four compactly shaped satellites, at an average altitude of about 200 km. There was a systematic difference of about ten percent between the two types of satellites. By using Sentman's model with physical parameters measured in orbit, it was possible to reduce this difference to three percent[17,18], and bring the measurements from both types of satellites to within three percent of the average density from 11 of the most recent density models. These results increase confidence that drag coefficients calculated from Sentman's model, using the parameters (accommodation coefficient and angular distribution) measured near 200 km, are accurate to about 3 % for satellites having smooth surfaces of typical compositions. The effects of unusual surface compositions and surface treatments are investigated in the companion paper[38].

The parameters used in drag coefficient models are the angular distribution of molecules reemitted from the satellite surface and the energy accommodation coefficient, which is a measure of the fraction of kinetic energy lost before the molecules are reemitted from the surface. Near 200 km, accommodation coefficients of 0.99 to 1.00 have been measured by Beletsky[19], and by Ching et al.[20], while angular distributions within a few percent of diffuse were reported by Beletsky[19], and by Gregory and Peters[21]; but at 325 km near sunspot minimum, Imbro et al.[15] measured an accommodation coefficient of 0.86 to 0.88. We don't know the amounts of atomic oxygen adsorbed on the satellite surfaces in these

particular cases, but we know from decades of satellite and laboratory measurements that atomic oxygen adsorbs on satellite surfaces and on nearly any material, and we know that it is continually adsorbing and desorbing[22-27]. We know from laboratory measurements that adsorbed molecules greatly increase the accommodation coefficients[28,29]. We therefore have used the atomic oxygen measurements collected in the monograph on the US Standard Atmosphere, 1976[30] to extrapolate the accommodation coefficient measurements, which were mostly made near sunspot minimum, to times of high solar activity, at which time there is much more atomic oxygen in the thermosphere. We also have used these oxygen measurements to extend the accommodation coefficients to altitudes above 325 km.

The orbital measurements indicate that at altitudes near 200 km, the molecules are reemitted diffusely with a high degree of energy accommodation. The energy accommodation coefficient, α, is defined as

$$\alpha = (E_i - E_r) / (E_i - E_w) \tag{1}$$

where E_i is the kinetic energy of the incident molecules, E_r is the kinetic energy of the reemitted molecules, and E_w is the energy that the reemitted molecules would have if they were reemitted at the surface (wall) temperature[31].

The analysis of the momentum transfer to the satellite, appropriate for the case of diffuse reemission, was developed by Sentman[9,10]. The resulting expression for the physical drag coefficient of a sphere is

$$\begin{aligned} C_{DP} = 1 + \frac{1}{2s^2} + (2 + \frac{1}{s^2}) \int_0^{\pi/2} \sin\theta \cos\theta \; erf(s\cos\theta)\, d\theta + \frac{2}{s\sqrt{\pi}} \int_0^{\pi/2} \sin\theta \; e^{-s^2\cos^2\theta}\, d\theta \\ + \frac{\sqrt{\pi} V_r}{V_i} \left[\frac{1}{3} + \int_0^{\pi/2} \sin\theta \cos^2\theta \; erf(s\cos\theta)\, d\theta + \frac{1}{s} \int_0^{\pi/2} \sin\theta \cos\theta \; e^{-s^2\cos^2\theta}\, d\theta \right] \end{aligned} \tag{2}$$

The parameter s is the speed ratio, defined as the velocity of the incident molecules divided by the most probable speed of the ambient atmospheric molecules. V_i is the speed of the incident molecules. V_r is the most probable speed of the reemitted molecules. It is related to α by

$$V_r = \sqrt{2/3}\, V_i \, [\, 1 + \alpha \, (\frac{T_w}{T_i} - 1)]^{1/2} \tag{3}$$

where T_i is the kinetic temperature corresponding to the incident velocity, and T_w is the temperature of the satellite surface (or wall).

Table 2 is presented to provide insight into the various physical contributions to the drag coefficient. It was calculated from Sentman's model, and applies to the case of diffuse reemission at a time of low solar activity. The first contribution, labeled "incident momentum", gives the contribution from the flux of incident particles, ignoring the

random thermal motions of the ambient air. The next column gives the contribution of the random motion, and the third contribution is the drag caused by the reemission of particles. The final column gives the physical drag coefficient of a sphere at a time of low solar activity, when the reemitted particles are assumed to have a completely diffuse angular distribution. Table 2 demonstrates the fact that the physical drag coefficient of a sphere at altitudes near 200 km must be above 2.00.

Altitude (km)	Alpha	Contributions to C_{DP}			C_{DP}
		Incident momentum	Random air motions	Reemitted momentum	
150	1.00	2.00	0.013	0.067	2.08
200	0.99	2.00	0.018	0.132	2.15
300	0.93	2.00	0.026	0.314	2.34

Table 2. Contributions to the physical drag coefficient C_{DP} when reemission is diffuse during sunspot minimum.

At altitudes above 300 km at solar minimum, there is a quasi-specular component of reemission[16] that becomes increasingly important as the altitude increases and the surface coverage of adsorbed atomic oxygen is reduced[27]. The effect of this component on C_{DP} is calculated in the companion paper[38]. The diffuse and quasi-specular contributions to C_{DP} at sunspot maximum and minimum are tabulated in the appendix of that paper. These values will be compared with the fitted drag coefficients, C_D , in the figures of the present paper.

C_D Analysis of Spherical Satellites

The decayed spherical satellites used in this analysis are listed in Tables 3 and 4, which include the physical and orbital characteristics.

The ODERACS spheres[32] were launched for radar calibration studies and decayed during the solar minimum period of 1994-1995. These small 4" and 6" spheres were excellent candidates for determining the drag coefficient variations resulting from different surface characteristics. The Starshine satellites were launched, and also decayed, in the 1999-2002 solar maximum time period. These satellites were used for optical tracking experiments. Starshine 1 and 2 had 68% of their surfaces covered by small mirrors, while Starshine 3, twice the diameter of the other two satellites, had only 30% of its surface made up of small mirrors, the other 70% covered with black chemglaze polyurethane paint. Also used in the analysis were three radar calibration Calspheres that decayed during solar maximum times of 1989-1990. In addition, 7 Russian Taifun radar calibration spheres were used in the analysis. The Taifun Yug class was passive hollow spheres with smooth surfaces. One of them decayed during solar minimum conditions, the other 3 decayed during solar maximum times of 1989-1990. The Taifun Type 2 spheres were covered with solar cells to provide power to the active transmissions for tracking purposes. Three of these satellites also decayed during the 1990 solar maximum period. Since the Taifun Type 2 and the Starshine satellites had numerous flat plates (mirrors or solar cells) attached to the spherical subsurface they cannot be considered true

spheres from the viewpoint of free-molecular aerodynamics. The final sphere used was GFZ-1, launched in 1995 and decayed four years later. Its surface included 60 large recessed mirrors used for laser ranging, and therefore also cannot be considered as a true aerodynamic sphere.

Satellite	Name	Dia	Mass	Sphere Surface	Incl	Launch Ht	Launch	Decay
		(m)	(kg)		(deg)	(km)		
04957	Calsphere 3	0.254	0.73	Aluminum	88.3	775	17-Feb-71	17-Oct-89
04958	Calsphere 4	0.254	0.73	Aluminum	88.3	775	17-Feb-71	20-Sep-89
04963	Calsphere 5	0.254	0.73	Gold	88.3	775	17-Feb-71	7-Jan-90
22990	ODERACS	0.1016	1.482	4" polished chrome	56.9	345	3-Feb-94	2-Oct-94
22991	ODERACS	0.1016	1.482	4" sand-blasted aluminum	56.9	350	3-Feb-94	4-Oct-94
22994	ODERACS	0.1524	5.000	6" polished chrome	56.9	350	3-Feb-94	3-Mar-95
22995	ODERACS	0.1524	5.000	6" sand-blasted aluminum	56.9	350	3-Feb-94	24-Feb-95
23471	ODERACS	0.1524	5.000	6" black iridite	51.9	340	3-Feb-95	13-Mar-96
23472	ODERACS	0.1016	1.482	4" white chemglaze	51.9	325	3-Feb-95	29-Sep-95
23558	GFZ-1	0.215	20.63	Recessed 60 reflectors	51.6	390	19-Apr-95	23-Jun-99
25769	Starshine 1	0.476	39.46	878 mirrors	51.6	380	5-Jun-99	18-Feb-00
26929	Starshine 3	0.934	90.04	1500 mirrors (30% covered)	67.0	470	30-Sep-01	21-Jan-03
26996	Starshine 2	0.476	38.56	845 mirrors	51.6	360	16-Dec-01	26-Apr-02

Table 3. Description of the satellites (non-Taifun), with their orbits, used for the C_D analysis.

Satellite	Taifun	Dia	Mass	Sphere Surface	Incl	Launch Ht	Launch	Decay
	Type	(m)	(kg)		(deg)	(km)		
11796	Yug	2.000	750+-10	Smooth surface	82.9	300	14-May-80	18-Jul-89
13750	Yug	2.000	750+-10	Smooth surface	65.8	450	29-Dec-82	5-Oct-89
15446	Yug	2.000	750+-10	Smooth surface	65.8	450	20-Dec-84	15-Apr-90
21190	Yug	2.000	750+-10	Smooth surface	65.8	450	19-Mar-91	3-Apr-95
13972	Type 2	2.007	750+-30	Covered with solar cells	65.8	470	6-Apr-83	30-May-90
14668	Type 2	2.007	750+-30	Covered with solar cells	65.8	470	26-Jan-84	19-Sep-90
15584	Type 2	2.007	750+-30	Covered with solar cells	65.8	470	27-Feb-85	8-Dec-90

Table 4. Description of the Taifun radar calibration spheres, with their orbits, used for the C_D analysis.

Determination of C_D Values

The same method used to validate the temperature field was used to compute the B values for the analyses of the decayed spheres. The daily temperature field correction equations were used in the special perturbation orbit fits to correct the atmospheric model. B values were then obtained each day using the optimum observation span based on the amount of observable drag. C_D values were then computed from the B values using the size and mass of each satellite listed in the above table.

ODERACS Radar Calibration Spheres

There were two separate launches (releases from the Space Shuttle) in 1994 and 1995 to place a number of radar calibration targets in orbit. This analysis used the three 4" and three 6" spheres included in the releases.

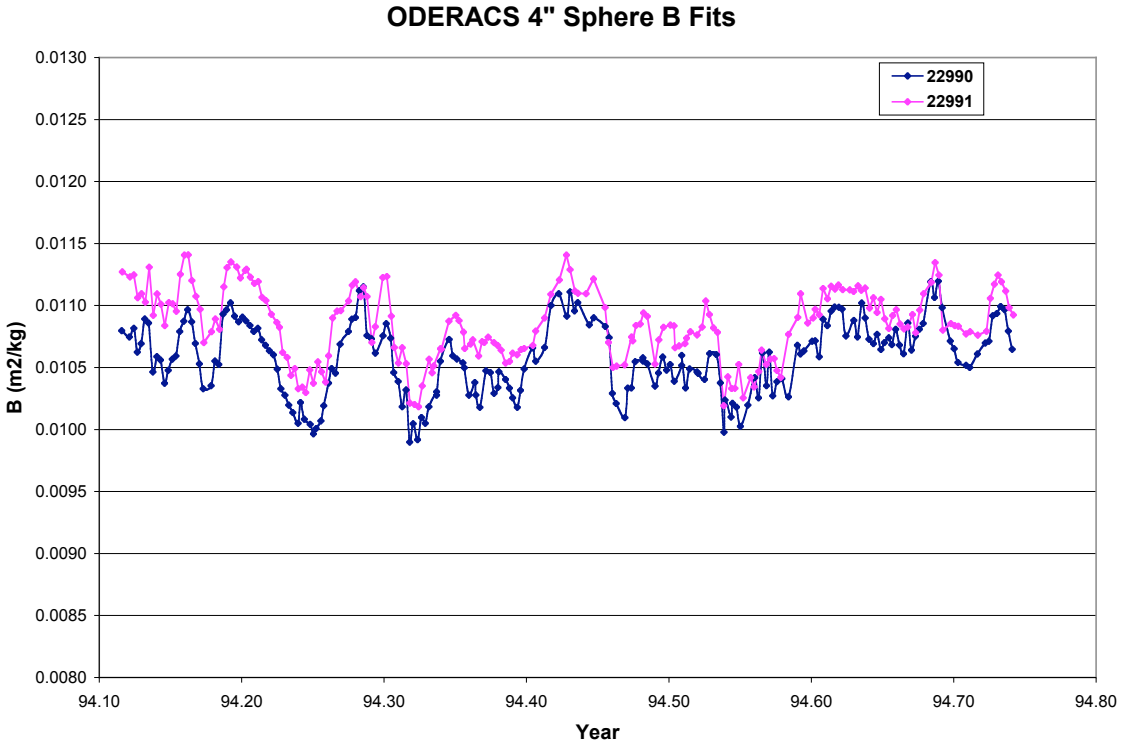

Figure 2. B values of two 4" ODERACS spheres placed in orbit during a 1994 Space Shuttle mission. Satellite 22990 had a polished chrome surface, while 22991 had a sandblasted aluminum surface.

Figure 2 shows the B values obtained after using the daily temperature corrections. The overall variations of approximately +-6% are the result of the remaining unmodeled density variations. What is notable is the almost constant difference between the two curves. The curves are almost identical because both spheres were released at almost the same time into almost identical orbits. Therefore, any unmodeled density variations will affect both spheres in the same way. The sandblasted surface appears to have an approximate 2% greater B value than the polished surface. This is discussed in more detail in a companion paper[38].

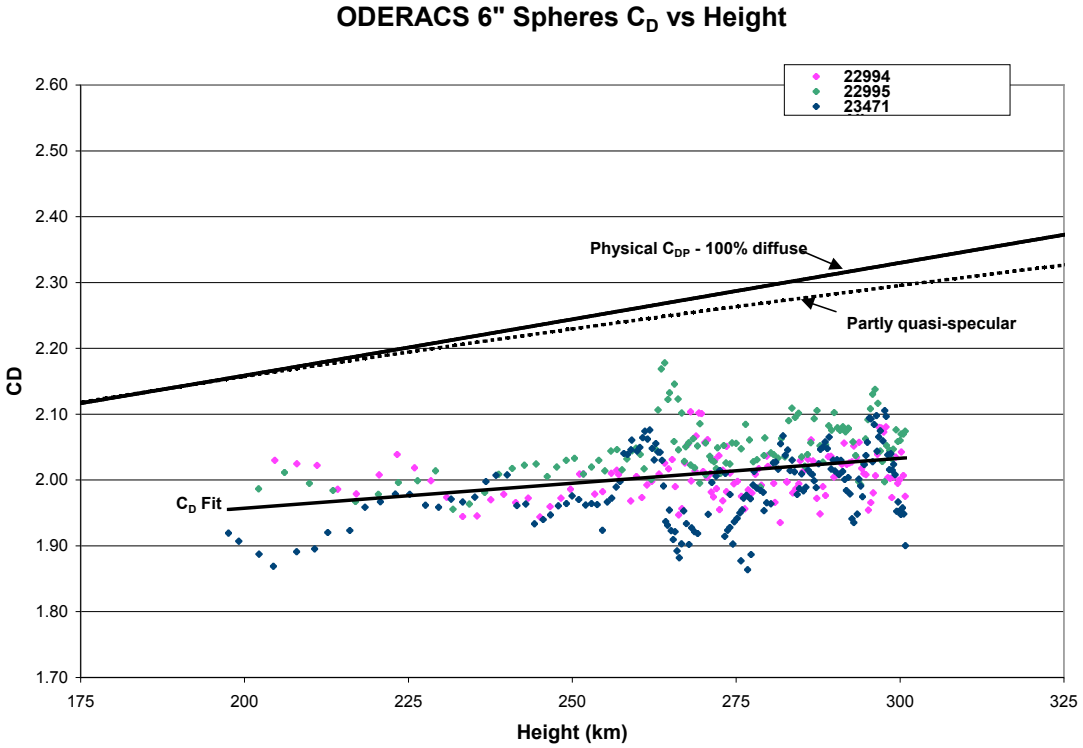

Figure 3. The C_D values for the ODERACS 6" spheres, plotted as a function of height.

Figure 3 shows the C_D values obtained for the three 6" spheres. The 22994 and 22995 spheres were released in 1994, while the 23471 sphere was released in 1995, a year later.

The 10% to 15% differences between the observed and computed drag coefficients are very significant. This difference, which is also observed later in the plots of the other spheres, will be discussed later. Table 5 lists the mean, standard deviation of the mean (Mean Sig), and % difference from that of sandblasted aluminum.

Satellite	Diameter	Surface	CD	Mean Sig	Delta CD %
				%	(-aluminum)
22991	4"	sand-blasted aluminum	1.99	0.2	-----
22990	4"	polished chrome	1.93	0.2	-3.0
23472	4"	white chemglaze	1.96	0.2	-1.5
22995	6"	sand-blasted aluminum	2.01	0.2	-----
22994	6"	polished chrome	1.96	0.2	-2.5
23471	6"	black iridite	1.97	0.2	-2.0

Table 5. Mean and standard deviation C_D values for the 4" and 6" ODERACS spheres. The mean C_D difference from the sand-blasted (aluminum) surface is also listed.

Starshine Spheres

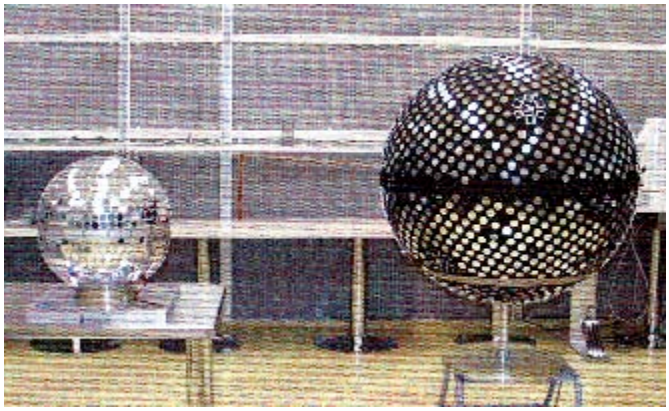

Figure 4. Starshines 2 (left) and 3 (right).

The second group of spherical satellites analyzed was Starshines. These three satellites were partly covered with small (1" diameter) flat mirrors to aid in optical tracking, so the Starshines are not true aerodynamic spheres. Starshine 1 and 2 were released into a near circular orbit, in 1999 and 2001 respectively, from the Space Shuttle. Starshine 3 was launched into a near circular orbit in 2001 from Kodiak Island. Starshine 1 and 2 were the same size, with approximately 850 1" diameter surface mirrors on a substrate of spun aluminum, and almost the same mass. Starshine 3 was twice as large in diameter as the other two, and had approximately 1500 1"diameter surface mirrors and 31 1"diameter laser reflectors on a substrate covered with black chemglaze polyurethane paint. The mirrors covered 68% of Starshine 1 and 2, but only 30% of Starshine 3. Figure 5 shows the computed C_D values for Starshine 1, obtained from the orbit fit B values, plotted as a function of perigee height over the last 100 days before decay.

The observed values are very close to the partly quasi-specular computed drag coefficient curve, although the observed values are still biased lower than the computed curves. The three Starshine satellites were expected to have very similar C_D values, even though Starshine 3 was larger and was launched into a higher orbit. Figure 6 shows the plot of C_D values for all three Starshine satellites. The observed values for Starshine 1 and 2 agree, while the larger Starshine 3 C_D values are lower than the computed curves by 10% to 15% depending on height. The main reason for the difference between Starshines 1 and 2 on the one hand and Starshine 3 on the other hand is that 68% of the surfaces of Starshines 1 and 2 were covered by small flat mirrors of circular cross section whereas 30% of the black paint surfaces of Starshine 3 were covered by the same kind of mirrors. The edges of the mirrors change the aerodynamic characteristics of the sphere. This is especially true near the edge of the sphere as viewed by the incident airstream. The C_D of Starshine 3 can be adjusted to the C_D of a sphere of black chemglaze polyurethane paint as will be explained in the companion paper[38]. The adjusted value of C_D is 1.90 which is plotted in Figure 6.

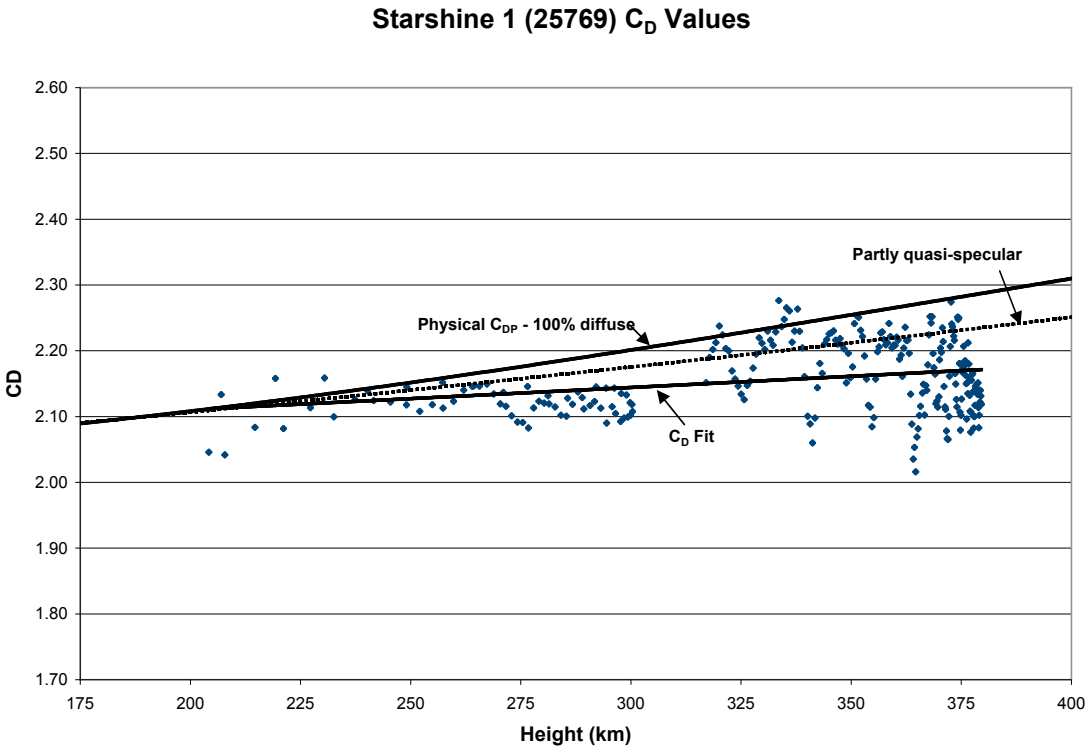

Figure 5. Plot of the C_D values of Starshine 1 as a function of height over the last 100 days of life.

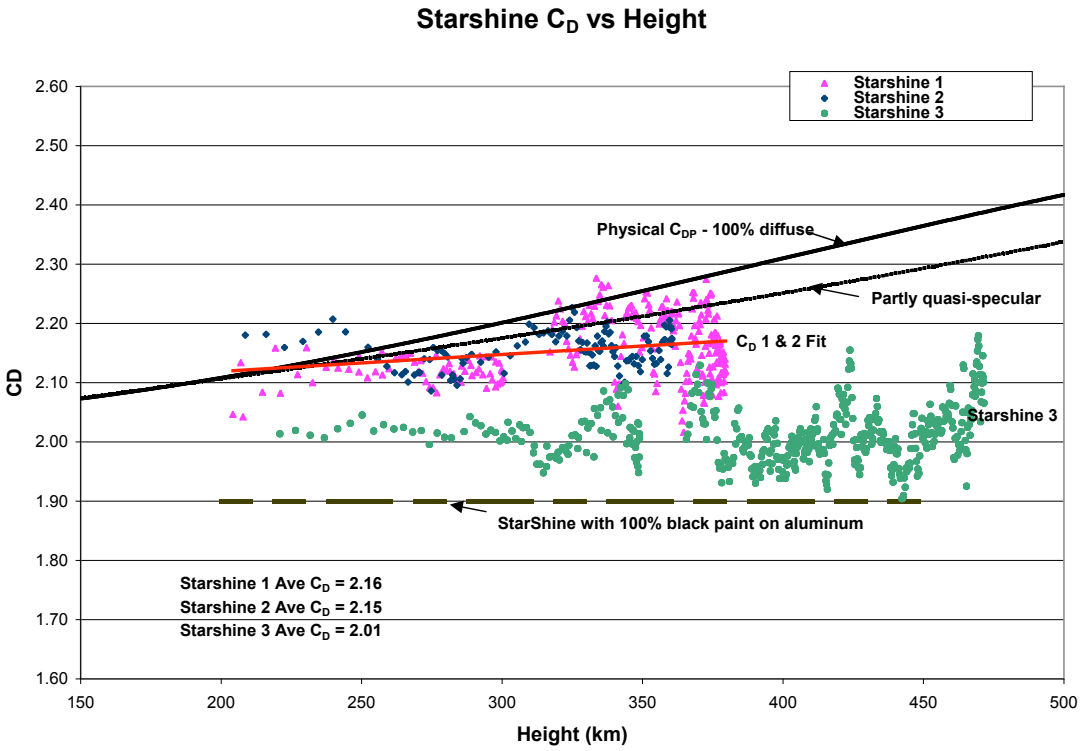

Figure 6. C_D values for the Starshine satellites, plotted as a function of height. The adjusted Starshine C_D values for 100% black paint on aluminum also are shown.

Taifun Radar Calibration Spheres

The Russians have launched many Taifun radar calibration spheres into orbit. One class of Taifun satellites, designated Yugs, was launched into either 300 km by 1600 km orbits, or nearly 450 km circular orbits. Four such Yugs were used in this analysis. One of them, 21190 decayed during solar minimum in 1995, and the other three Yugs decayed during solar maximum in 1989-1990. The Yug satellites are passive and hollow, with a smooth surface. The second class of Taifuns used in the analysis was the Type 2 active radar calibration spheres. This class of satellites had almost the identical size and mass of the Yugs, the only real difference being the surface of the Type 2 satellite was completely covered with solar cells. Since solar cells are flat plates, the Type 2 "spheres" were not true aerodynamic spheres. The diameters of the Yugs and Type 2 spheres were 2.000m+-0.010m and 2.007m+-0.010m respectively, with masses of 750kg+-10kg and 750kg+-30kg respectively[33].

Figure 7 shows the C_D values computed from the orbit fits of the Yug satellites. Theoretical curves for the quasi-specular C_{DP} values are shown for solar minimum and solar maximum conditions. The three Yugs that decayed in the solar maximum 1989-1990 period have C_D values consistently lower than the values observed for 21190, which decayed during solar minimum year 1995. This is consistent with theory; however, all the C_D values are significantly lower than the computed theoretical values, the same results observed for the ODERACS spheres described above. Figure 8 shows the C_D values observed for the Type 2 spheres. What is significant is the much closer agreement with the theoretical values than the agreement observed with the Yug spheres. Again, the only difference between the Type 2 and Yug satellites is that the surface of the Type 2 is completely covered with solar cells. The results for the Type 2 C_D values are much more consistent with the results obtained from Starshine 1 and 2, which were both 68% covered with mirrors. All these anomalous cases involved flat mirrors or flat solar cells, so the satellite surface was not strictly spherical. These results will be discussed later in the discussion section below and in the companion paper[38].

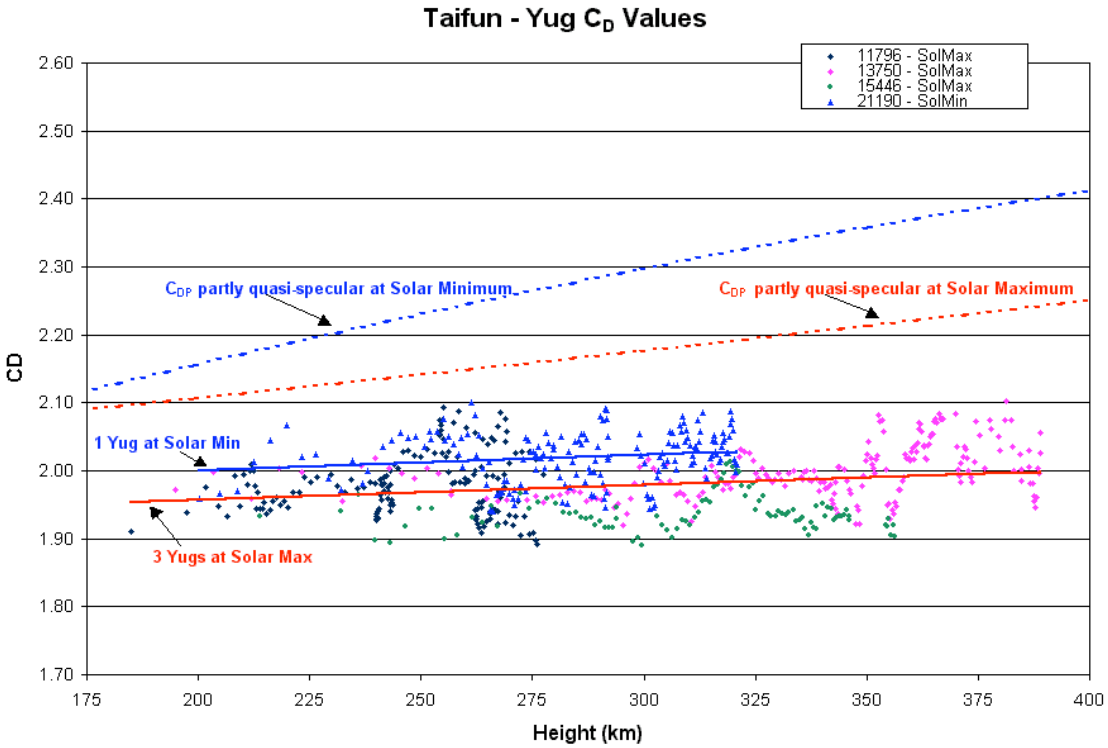

Figure 7. C_D values for Yug true spheres plotted as a function of altitude. Theoretical partly quasi-specular C_{DP} values are shown for solar minimum and maximum conditions.

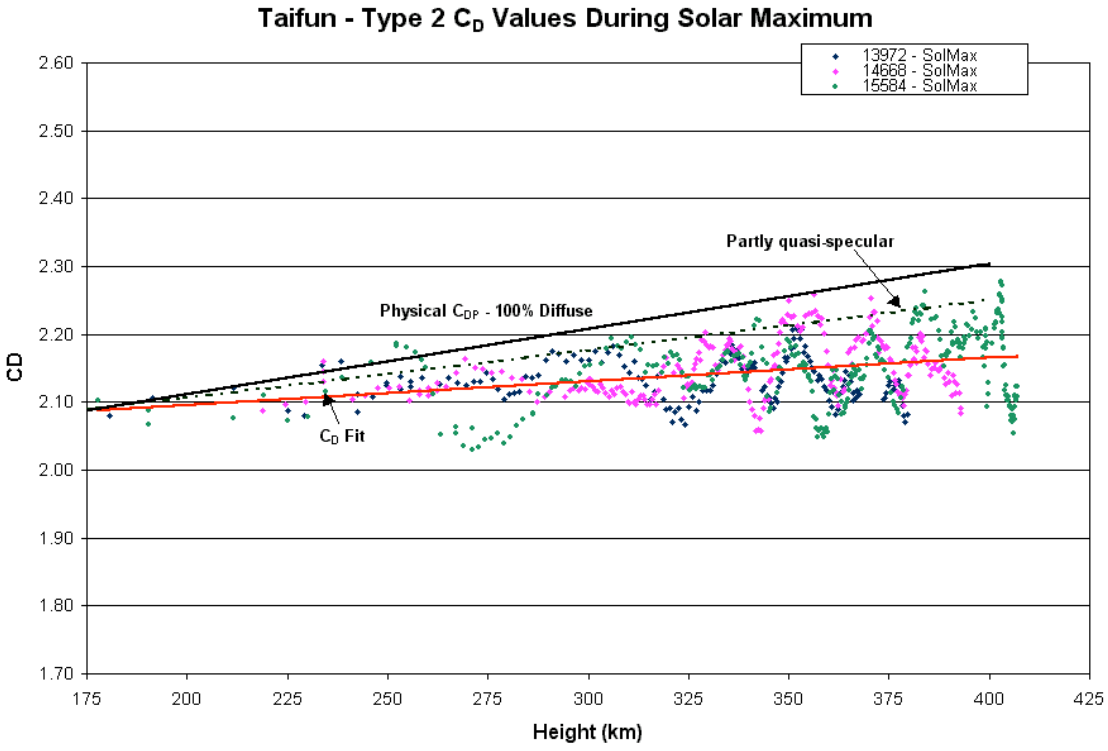

Figure 8. C_D values for three Taifun Type 2 modified spheres are plotted as a function of altitude. Also shown are theoretical C_{DP} values for 100% diffuse and partly quasi-specular conditions.

Calsphere Radar Calibration Spheres

Calspheres 3, 4, and 5 were all launched together in early 1971 into a circular 775 km polar orbit. They all decayed near the time of sunspot maximum in the late 1989 early 1990 time frame. King-Hele[34] lists the masses as 0.73 kg each, with diameters of 0.26m (10.2") each. He also lists the surface as aluminum for Calsphere 3 and 4, and gold for 5. The diameters of other radar calibration spheres are normally even increments of inches, so it was decided to use a 10.0" diameter for these spheres. It should be noted that density corrections were determined for 1989 using approximately 50 satellites that were a subset of the 79 satellites used for the 1994 through 2003 analyses. Figure 9 is a plot of all three sphere's C_D values as a function of perigee height. Because of the lightness of the spheres their decay was very rapid once the perigee height fell below 500 km. Figure 9 represents the decay during the last 100 days of lifetime. There are no data points below 300 km because it took less than 24 hours for them to decay from a circular orbit of 300 km.

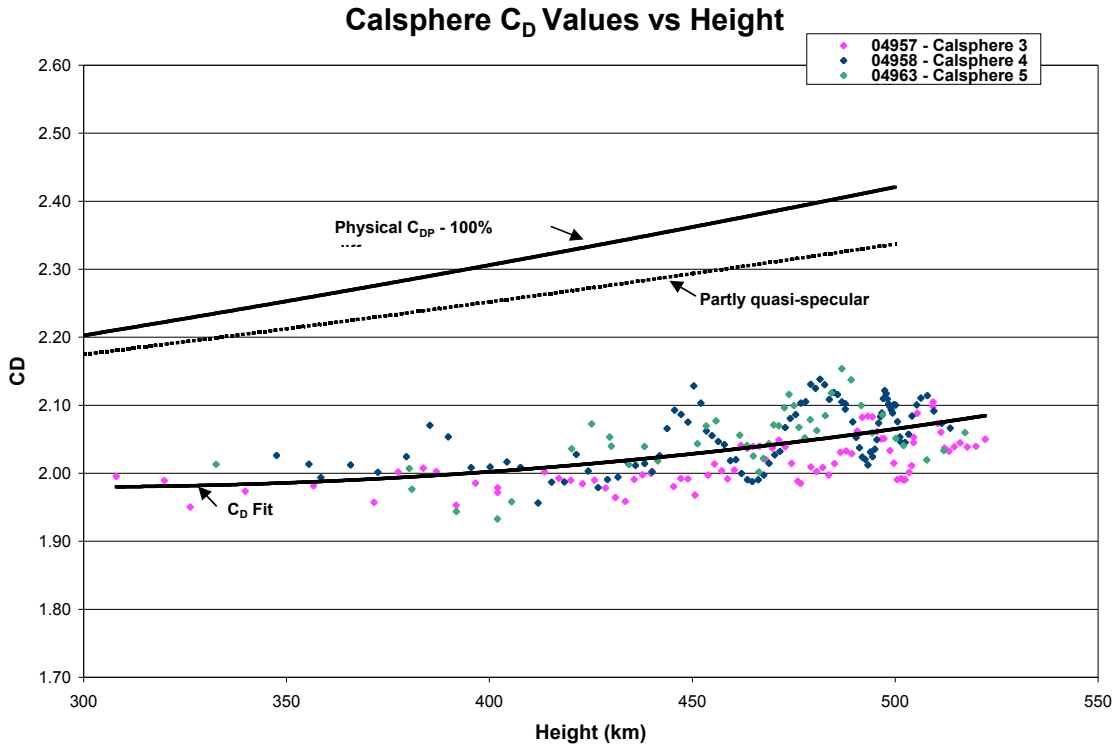

Figure 9. C_D values for Calspheres 3 through 5, plotted as a function of height.

GFZ-1 Sphere

GFZ-1 was a geodetic satellite designed to improve the current knowledge of the Earth's gravity field. The satellite was covered with recessed retroreflectors for laser beam tracking. GFZ-1 was deployed from the MIR space station into a circular orbit in 1995, and finally decayed in 1999. The satellite consisted of a spherical body made from brass with 60 corner cube reflectors distributed regularly over the satellite's surface. These retroreflectors were quartz prisms placed in special holders that were recessed in the satellite's body. External metallic surfaces were covered with white paint for thermal control purposes and to facilitate visual observation in space. Figure 10 is a picture of the satellite.

Figure 10. GFZ-1

Figure 11 shows plots of the B values and height of the circular orbit obtained for the GFZ-1 satellite. The computed C_D values have a standard deviation of 2.5% about the quadratic curve shown in Figure 12. The larger errors observed in the data near the higher altitudes is due to the fact that the orbit height remained at these higher altitudes for a much longer time than when the orbit was rapidly dropping, as displayed in Figure 11. At the higher altitudes, when the height was almost constant, the error is mainly due to the unmodeled density field error of approximately 4%. The small standard deviation of the C_D values indicates the high accuracy of the orbit fits.

It is initially surprising that the C_D values at 350 to 375 km are as high as 2.7. Secondly, it is also surprising that the C_D drops as rapidly as it does, down to a value of 1.80 at 175 km. The reason is due to the fact that the 60 laser reflectors are recessed into the surface of the sphere, which produce an effective drag similar to a cylinder flying endwise into the atmosphere. Therefore, GFZ-1 definitely cannot be used as a sphere for computing density values. All of the modified spheres will be studied in the companion paper[38].

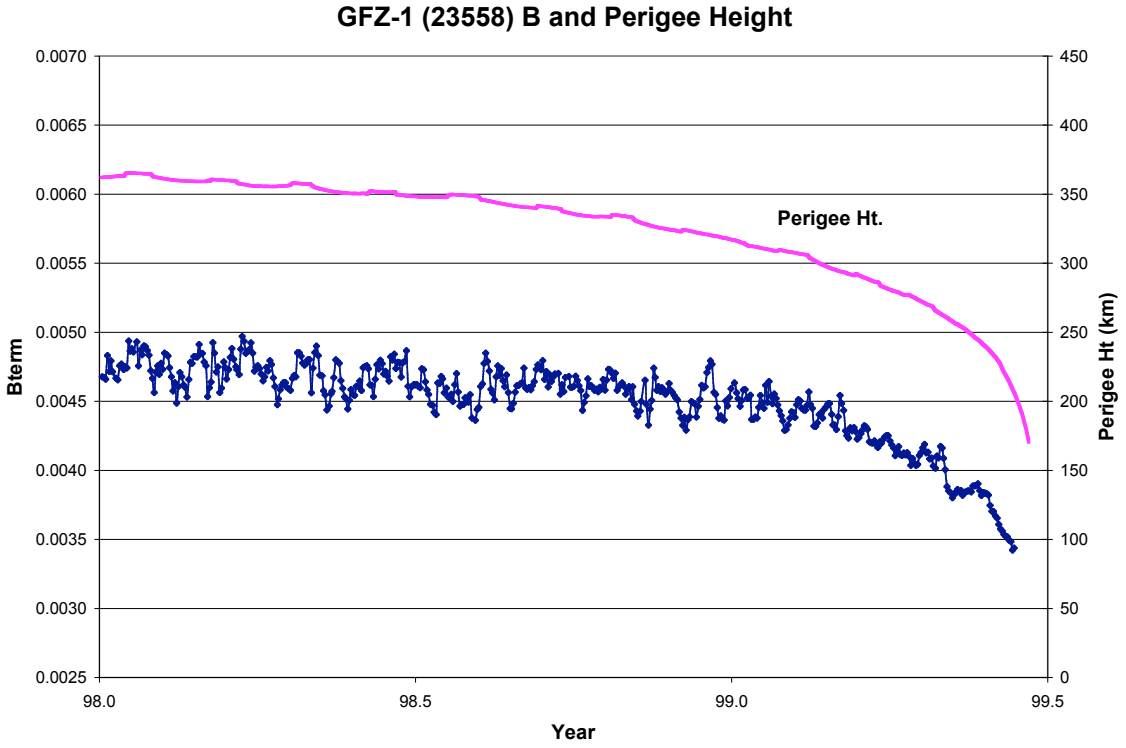

Figure 11. B values and perigee heights of GFZ-1 sphere during the last 1.5 years of orbit life.

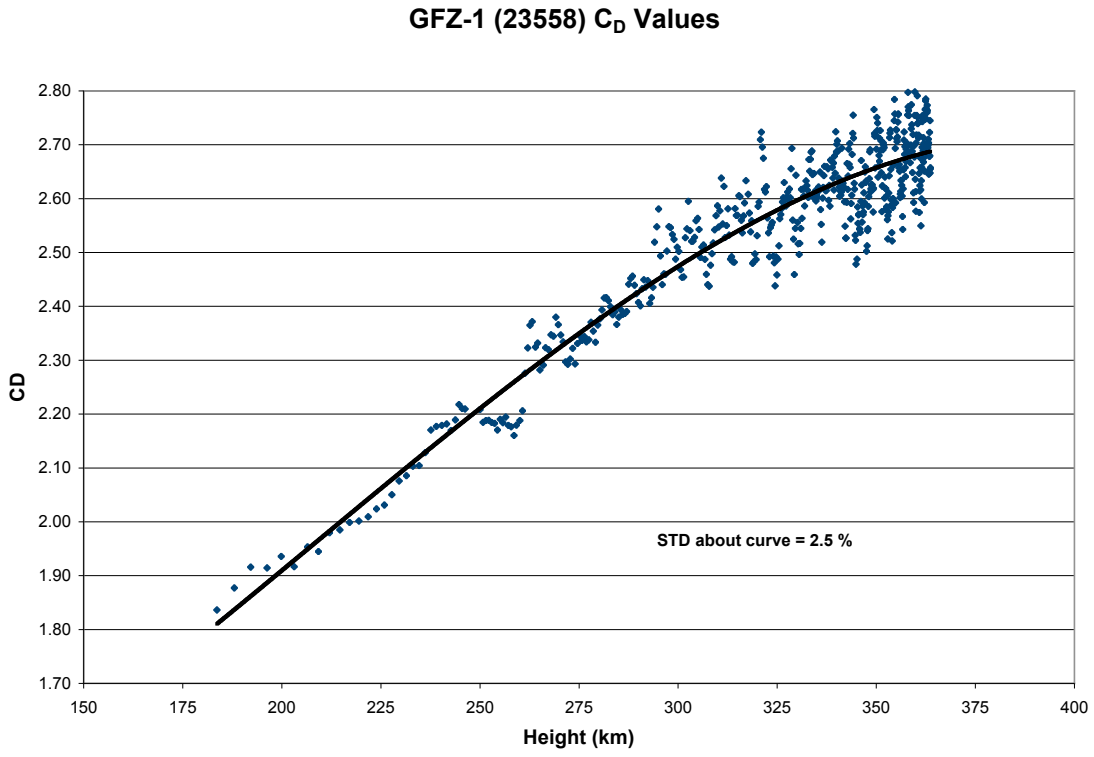

Figure 12. C_D values computed for the GFZ-1 satellite as a function of height.

Discussion

The observed drag coefficient differences from the theoretical values ($C_D - C_{DP}$) are shown in Figure 13 for all normal spheres. Part of the differences at 200 km may be caused by inaccuracies in the calculated physical drag coefficients. These may be corrected as more spheres are studied. The increasing divergences as the altitude increases reflects the increasing influence of surface composition as adsorption decreases.

The aerodynamic non-spheres Starshine 1 and 2, GFZ-1, and the Type 2 Taifun satellites have serious aerodynamic problems for a sphere. From the previous figures it has been clearly demonstrated that these satellites, covered either with flat plates of mirrors or solar cells, or recessed laser reflectors, do not behave as normal aerodynamic spheres behave. Therefore, they have not been included in Figure 13.

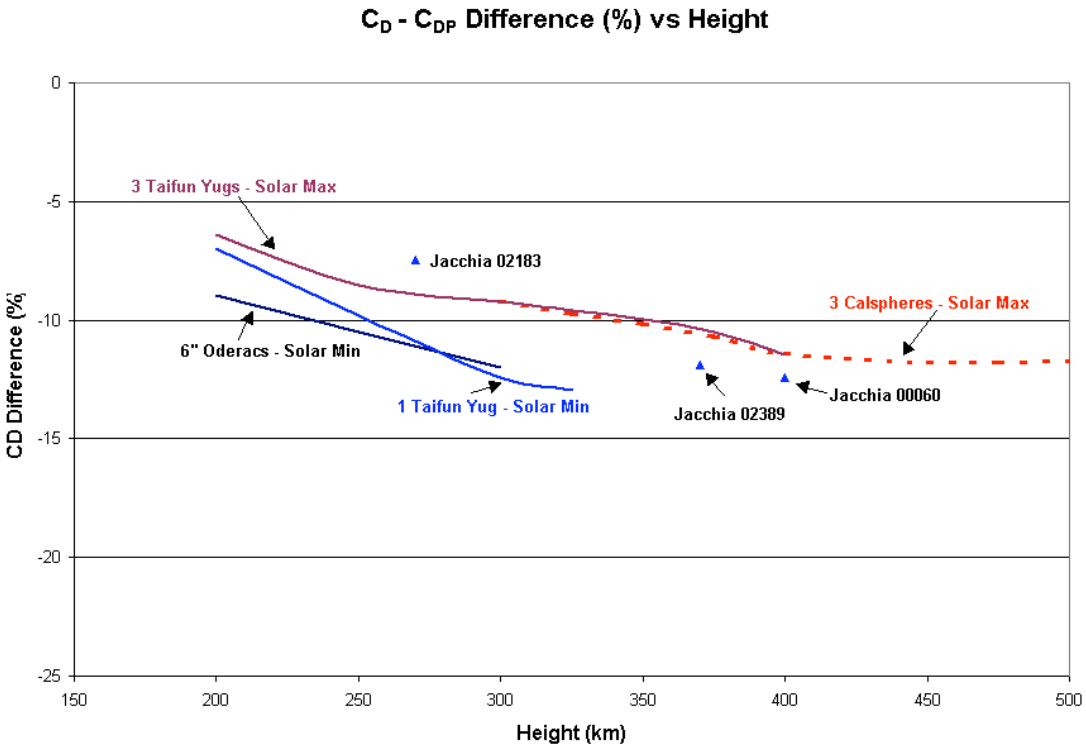

Figure 13. C_D difference values are obtained from comparing the observed C_D values against the computed C_{DP} values. The difference values, in percent, are plotted as a function of height.

From the previous physical drag coefficient discussion, the physical drag coefficients of spheres that have conventional surfaces have been firmly established with an uncertainty close to 3 % at 200 km. We therefore infer from Figure 13 that the Jacchia model[7] is about 8 % high at 200 km, and about 12-13% high at 500 km at sunspot maximum.

This bias in the Jacchia 70 model can also be observed from analyzing some of the data used by Jacchia to develop the model. Most of his density data[35] was obtained from drag analysis of satellites during the 1965-1969 solar minimum time period. Three of the satellites he used extensively are listed in Table 6. The B that Jacchia used for each satellite is listed in the table, as well as the average (Ave) B obtained from fitting special perturbation B values over 15 to 30 years of daily values[36] obtained from using the

Jacchia 70 model atmosphere. If his atmospheric model represented his B values over the complete 11-year solar cycle then the average 15-30 year B values should agree with his B values used to compute the model. However, the average B values are all ~6% too low, which implies that his density model is ~6% too high, a result of using data covering only a partial 11-year solar cycle. In addition, he used a C_D value of 2.2 for satellite orbits under 400 km, which would produce an additional density error not observed by the average 15-30 year B values. Table 6 compares the correctly computed B values, obtained from using the theoretical partly quasi-specular C_D values, with the average 15-30 year B values obtained from the Jacchia 70 model. The C_D differences for these satellites are plotted in Figure 13. The differences are in excellent agreement with those obtained from the sphere data. The average B values are 8 to 13% low, depending upon height, from the computed theoretical values. This means that the Jacchia 70 model density values are too high by 8-13% for these heights in order to match the observed historical drag values. This bias is also confirmed from the results reported in the AIAA American National Standard[37] that states, under model uncertainties, that "available data on average total densities obtained from mass spectrometer data are approximately 10 percent lower" than the Jacchia 70 atmospheric model.

Sat	Name	Type	Ht (km)	Jacchia A/M	Jacchia C_D	Jacchia B	True B	D B % Jacchia	True C_D Quasisp	Comp B	D B % Comp
02183	Exp 32	Sphere	270	0.00299	2.20	0.00658	0.00615	-6.5	2.21	0.00661	**-7.4**
02389	OV3-3	Cyl	370	0.00870	2.20	0.01914	0.01796	-6.2	2.31	0.02010	**-11.9**
00060	Exp 8	Dbl cone	400	0.01100	2.20	0.02420	0.02290	-5.4	2.34	0.02574	**-12.4**

Table 6. B values obtained from Jacchia, 15-30 year averages (Ave B), and theoretical computed values (Comp B). The D B % Comp column compares the computed with the long term Ave B values.

Summary

Jacchia-type static diffusion models are widely used. This has led to many past efforts to evaluate and improve these models. New orbit fitting data reduction methods have greatly improved the precision of the Jacchia 70 atmospheric density model. Here density corrections to the improved Jacchia model have been used with tracking data from numerous spherical satellites to compute accurate fitted drag coefficients. Furthermore, physical drag coefficients have been calculated from parameters of gas-surface interaction previously measured in orbit. Comparison of the two types of drag coefficient has made it possible to remove from the atmospheric model the bias caused by Jacchia's original assumption that the physical drag coefficient of compact satellites is 2.2 at all altitudes. The most likely physical drag coefficients of spheres at sunspot maximum and minimum have been included in several of the graphs. These provide the basis for obtaining the density correction factors provided in Table 7. The improved drag coefficients will also facilitate improved density measurements and models, thus contributing to the long-term Air Force effort to improve orbital predictions.

Ht (km)	200	250	300	350	400	450	500
Rho Bias %	7-8 %	9-10 %	11-12 %	11-12 %	12-13 %	12-13 %	12-13 %

Table 7. Jacchia 70 atmospheric model density bias as a function of height.

Acknowledgments

We would like to thank the following people for providing satellite details: Susan Andrews, ODERACS Historian, MIT Lincoln Laboratory, for ODERACS information; Gil Moore, Director of Project Starshine, for Starshine information; and Vladimir Agapov, Russian Space Agency, for detailed Taifun information. We would also like to thank Robin Thurston (USAF/AFSPC) and Bill Schick (Omitron, Inc.) for supplying the USAF Space Surveillance Network satellite observations. We also thank Steven W. Wallace for programming the numerical evaluation of equation (2).

References

1. Bowman, B. R., and Storz, M.F., 2003. High Accuracy Satellite Drag Model (HASDM) Review, AAS 2003-625, AAS/AIAA Astrodynamics Specialist Conf., Big Sky, Mt, August.
2. Marcos, F. A., 1985. Requirements for improved thermospheric neutral density models, AAS Paper 85-312, AAS Publications Office, P. O. Box 28130, San Diego, CA 92128.
3. Chao, C. C., Gunning, G. R., Moe, K., Chastain, S. H., and Settecerri, T. J., 1997. An evaluation of Jacchia 71 and MSIS 90 atmosphere models with NASA ODERACS decay data, J. Astronautical Sci., Vol. 45, No. 2, pp.131-141.
4. Owens, J. K., 2002. NASA Marshall Engineering Thermosphere Model, Version 2.0, NASA/TM-2002 -211786, Marshall Space Flight Center, MSFC, AL.
5. Wise, J. O., Marcos, F. A., Kendra, M., Bass, J., and Bowman, B., 2003. A statistical evaluation of the MET model for total density prediction, AIAA Paper -2003-569.
6. Bowman, B.R., 2004. The Semiannual Thermospheric Density Variation From 1970 to 2002 Between 200-1100 km, AAS 2004-174, AAS/AIAA Spaceflight Mechanics Meeting, Maui, Hi, February. .
7. Jacchia, L.G., 1971. Revised Static Models of the Thermosphere and Exosphere with Empirical Temperature Profiles, Smithson. Astrophys. Special Report 332.
8. Bowman, B.R., , Marcos, F. A., Kendra, M., 2004. A Method for Computing Accurate Daily Atmospheric Density Values from Satellite Drag Data, AAS 2004-179, AAS/AIAA Spaceflight Mechanics Meeting, Maui, Hi, February.
9. Sentman, L. H., 1961. Free molecule flow theory and its application to the determination of aerodynamic forces. Lockheed Missile and Space Co., LMSC-448514, AD 265-409, Sunnyvale, CA, Available from National Technical Information Service, Springfield, VA.
10. Sentman, L. H., 1961. Comparison of the exact and approximate methods for predicting free molecule aerodynamic coefficients, ARS J., 31, 1576 -1579.
11. Schamberg, R., 1959a. A new analytic representation of surface interaction for hyperthermal free molecular flow, Rand Corp., RM-2313, Santa Monica, CA.
12. Schamberg, R., 1959b. Analytic representation of surface interaction for free molecular flow with application to drag of various bodies. Aerodynamics of the Upper Atmosphere, Rand Corp., R-339, Santa Monica, CA, 12-1 to 12-41.
13. Bruce, R. W., 1973. Upper atmosphere density determination from LOGACS, in The low-G accelerometer calibration system, Vol. 1, Rept. TR-0074 (4260-10) - 1, Vol. 1, The Aerospace Corp., El Segundo, CA.
14. DeVries, L. L., Schusterman, L., and Bruce, R. W., 1972. Atmospheric density variations at 140 km deduced from precise satellite radar tracking data, J. Geophys. Res., April, 1972.
15. Imbro, D. R., Moe, M. M., and Moe, K., 1975. On fundamental problems in the deduction of atmospheric densities from satellite drag, J. Geophys. Res., Vol 89, pp. 3077-3086.
16. Moe, K., Moe, M. M., and Wallace, S. D., 1996. Drag coefficients of spheres in free- molecular flow, AAS Paper 96-126, AAS Publications Office, P. O. Box 218130, San Diego, CA 92198.
17. Moe, K., Moe, M. M., and Wallace, S. D., 1998. Improved satellite drag coefficient calculations from orbital measurements of energy accommodation. J. Spacecraft and Rockets, 35, 266-272.
18. Moe, K., Rice, C.J., and Moe, M. M., 2004. Simultaneous analysis of multi-instrument satellite measurements of atmospheric density. J. Spacecraft and Rockets, Vol. 41, No. 5, Sept.–Oct., pp. 849-853.

19. Beletsky, V. V., 1970. An estimate of the character of the interaction between the airstream and a satellite. (in Russian) Kosmicheskie Issledovaniya, 8, 206.
20. Ching, B. K., Hickman, D. R., and Straus, J. M., 1977. Effects of atmospheric winds and aerodynamic lift on the inclination of the orbit of the S3-1 Satellite. J. Geophys. Res. 82, 1474-1480.
21. Gregory, J. C., and Peters, P. N., 1987. A measurement of the angular distribution of 5 eV atomic oxygen scattered off a solid surface in earth orbit. Proceedings of the 15th International Symposium on Rarefied Gas Dynamics, Vol. 2, B. G. Teubner, Stuttgart, Germany. 644-654.
22. Wood, B. J., 1971. The rate and mechanism of interaction of oxygen atoms and hydrogen atoms with silver and gold, J. Phys. Chem.., Vol. 75, pp. 2186-2193.
23. Riley, J. A. and Giese, C. F., 1970. Interaction of atomic oxygen with various surfaces, J. Chem.Phys., Vol. 53, pp. 146-152.
24. Lake, L. R. and A. O. Nier, 1973. The loss of atomic oxygen in mass spectrometer ion sources, J. Geophys. Res., Vol. 78, pp. 1645-1653.
25. Moe, M. M. and Moe, K., 1969. The roles of kinetic theory and gas-surface interactions in measurements of upper-atmospheric density. Planet. Space Sci. 17, 917-922.
26. Hedin, A. E., Hinton, B. B., and Schmitt, G. A., 1973. Role of gas-surface interactions in the reduction of OGO 6 neutral particle mass spectrometer data. J. Geophys.Res. 78, 4651-4668.
27. Offermann, D., and Grossmann, K.U., 1973. Thermospheric density and composition as determined by a mass spectrometer with cryo ion source. J. Geophys. Res. 78, 8296-8304.
28. Thomas, L. B., 1980. Accommodation of molecules on controlled surfaces. Rarefied Gas Dynamics, Proc. 12th Symposium.
29. Saltsburg, H., Smith, J. N.., Jr., and Rogers, M. (eds.), 1967. Fundamentals of gas-surface interactions. Academic, New York, passim.
30. NOAA, NASA, and USAF, 1976. US Standard Atmosphere, 1976.
31. Trilling, L., 1967. Theory of gas-surface collisions, pp. 392-421 in ref. 29.
32. Cress, G. H., Potter, A. E., Settecerri, T. J., Sherrill, G. P., Stansbery, E. G., and Talent., D. L., 1996. Radar and Optical Ground Measurements Final Report, Orbital Debris Radar Calibration Spheres, NASA Report JSC-27242, NASA Johnson Space Center, Houston, TX.
33. Agapov, Vladimir, 2000, Russian Space Agency, private communication.
34. King-Hele, D.G., etc., 1990. The R.A.E. Table of Earth Satellites 1957-1989," Royal Aerospace Establishment, Farnborough, England.
35. Jacchia, L.G., Slowey, J.W., 1973. A Supplemental Catalog of Atmospheric Densities From Satellite-Drag Analysis, Smithson. Astrophys. Special Report 348.
36. Bowman, B.R., 2002. True Satellite Ballistic Coefficient Determination for HASDM, AIAA 2002-4887, AAS/AIAA Astrodynamics Specialist Conf., Monterey, Ca, August.
37. AIAA, 2004, Guide to Reference and Standard Atmospheric Models, G-003B-2004, 2004 American Institute of Aeronautics and Astronautics, p 44.
38. Moe, K., Bowman, B.R., 2005. The Effects of Surface Composition and Treatment on Drag Coefficients of Spherical Satellites, AAS 2005-258, AAS/AIAA Astrodynamics Specialist Conf., Lake Tahoe, CA, August.